

## Reductive Cleavage of the N–N Bond: Synthesis of Imidoiron(III) Cubanes

Atul K. Verma and Sonny C. Lee\*

Department of Chemistry, Princeton University  
Princeton, New Jersey 08544

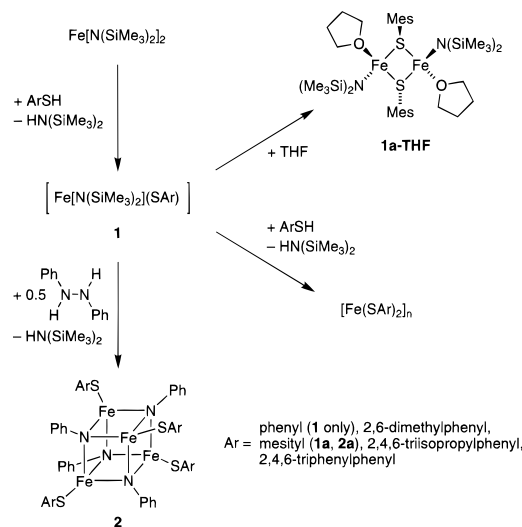
Received June 14, 1999

The biological reduction of dinitrogen to ammonia is mediated by a unique metal–sulfur cluster (FeMo–cofactor) within the enzyme nitrogenase.<sup>1</sup> Despite extensive study, the molecular mechanism of biological nitrogen fixation remains unresolved. The crystal structure of the catalytic component of this enzyme system (MoFe–protein) has provided a visualization of resting state FeMo–cofactor as a [MoFe<sub>7</sub>S<sub>9</sub>] cluster core.<sup>2</sup> This structural model has inspired renewed speculation about the molecular details of nitrogenase action,<sup>3</sup> including proposals where dinitrogen binding and reduction occur via bridging interactions to multiple iron sites at the cluster center.<sup>4</sup> These mechanisms implicate the intermediacy of new types of iron–sulfur (Fe–S) clusters which incorporate nitrogen atoms as cluster core ligands both before and after reductive scission of the N<sub>2</sub> substrate.

Although these hypothetical iron-binding models have been extensively investigated by computation,<sup>3b,4</sup> supporting experimental data are limited. We seek to address this issue by exploring the fundamental reaction chemistry of Fe–S complexes with N<sub>2</sub> fragments at various redox levels. We report here an Fe(II)–S mediated reductive N–N bond cleavage, with consequent assembly of a ferric imide thiolate cluster (Scheme 1).

Reaction of light green Fe[N(SiMe<sub>3</sub>)<sub>2</sub>]<sub>2</sub><sup>5</sup> with 1 equiv of aryl thiol (ArSH) in benzene generates a dark red solution of species with putative empirical formulation Fe[N(SiMe<sub>3</sub>)<sub>2</sub>](SAr) (**1**).<sup>6</sup> Although well-defined samples of **1** have proven difficult to isolate from the reaction medium, crystallization of the mesitylthiol (MesSH) derivative (**1a**) in the presence of THF gives orange-yellow crystals of the heteroleptic dimer, [Fe{N(SiMe<sub>3</sub>)<sub>2</sub>}(μ-SMes)(THF)]<sub>2</sub> (**1a-THF**). Protonolysis of amide thiolate **1** with a second equivalent of thiol yields a brick-red precipitate of homoleptic ferrous thiolate, [Fe(SAr)<sub>2</sub>]<sub>n</sub>. For Ar = 2,4,6-triphenylphenyl (Triph), dimeric [Fe(μ-STriph)(STriph)]<sub>2</sub><sup>7</sup> is the stable form; in contrast, homoleptic complexes with less hindered aryls (e.g., Ar = mesityl) are probably coordination polymers in

## Scheme 1



the solid state, as evidenced by their very limited solubility in all but the most polar coordinating solvents (DMF, DMSO).<sup>8</sup>

Single-crystal X-ray diffraction analysis of **1a-THF** reveals a centrosymmetric ferrous dimer (Figure 1).<sup>9a</sup> The distorted tetrahedral iron sites possess terminal amido and THF ligation, and are bridged asymmetrically by pyramidal thiolato sulfurs to form an [Fe<sub>2</sub>S<sub>2</sub>] rhomb typical in Fe–S coordination chemistry.<sup>10–12</sup> Analogous heteroleptic ferrous amide thiolate complexes with bulkier ligands have been characterized as either dimers<sup>12</sup> or monomers<sup>13</sup> with low-coordinate iron sites. Complex **1a-THF** establishes an Fe–S environment in conjunction with a reactive amide ligand that can be substituted readily and selectively by protonolysis.

Treatment of **1a** (1 equiv, generated in situ in benzene) with 0.5 equiv of 1,2-diphenylhydrazine results in an instantaneous deepening of solution color from dark red to maroon. After being stirred for 20 h, the solution is filtered, concentrated, treated with *n*-pentane, and cooled to –20 °C to give [Fe<sub>4</sub>(μ<sub>3</sub>-NPh)<sub>4</sub>(SMes)<sub>4</sub>]

(6) (a) The mesitylthiolate derivative **1a** displays a complex, paramagnetic <sup>1</sup>H NMR spectrum in C<sub>6</sub>D<sub>6</sub> with no evidence of the homoleptic bis(amide) or bis(thiolate) species. In d<sub>8</sub>-THF, **1a** exhibits a simplified NMR spectrum identical with that obtained from crystalline **1a-THF**. For the very hindered Ar = Triph analogue, the <sup>1</sup>H NMR spectrum is well-defined<sup>6b</sup> and consistent with the formation of a heteroleptic species, presumably [Fe(μ-STriph)-N(SiMe<sub>3</sub>)<sub>2</sub>]<sub>2</sub>.<sup>6c</sup> (b) See Supporting Information. (c) The selenium analogue, [Fe(μ-SeTriph){N(SiMe<sub>3</sub>)<sub>2</sub>]<sub>2</sub>, has been crystallographically characterized: Hauptmann, R.; Kliss, R.; Henkel, G. *Angew. Chem., Int. Ed.* **1999**, *38*, 377.

(7) Senge, K. R.; Power, P. P. *Bull. Soc. Chim. Fr.* **1992**, *129*, 594.  
(8) The <sup>1</sup>H NMR spectrum of [Fe(SMes)<sub>2</sub>]<sub>n</sub> in d<sub>6</sub>-DMSO is consistent with a paramagnetic complex bearing two different thiolate sites in a 1:1 ratio, perhaps the solvent coordinated dimer [Fe(μ-SMes)(SMes)(DMSO)]<sub>2</sub>. <sup>1</sup>H NMR (500 MHz, d<sub>6</sub>-DMSO, 293 K): δ 36.17 (3 H, *p*-Me), 35.72 (3 H, *p*-Me), 35.20 (6 H, *o*-Me), 33.87 (6 H, *o*-Me), 26.58 (2 H, *m*-Mes), 25.91 (2 H, *m*-Mes).

(9) Crystal data (Mo Kα) are given as *a*, *b*, *c* (Å); α, β, γ (deg); space group, *Z*, *T* (K); 2θ<sub>min/max</sub> (deg), unique/observed [*I* > 2σ(*I*)] data, *R*<sub>1</sub>/*wR*<sub>2</sub> for observed data (%), GooF. (a) **1a-THF**: 10.4231(3), 10.9167(5), 12.8489(5); 66.488(2), 69.768(2), 85.210(2); *P*<sub>1</sub>, 1, 200(2); 4.2/54.7, 5666/4047, 4.64/11.52, 1.025. (b) **2a·1.5C<sub>6</sub>H<sub>6</sub>**: 15.2729(7), 18.6174(7), 23.6395(10); 105.922(2), 96.730(2), 93.088(2); *P*<sub>1</sub>, 4, 170(2); 2.3/46.0, 17699/10168, 5.91/9.27, 1.022.

(10) Selected distances (Å) and angles (deg) for related structures. (a) [Fe<sub>2</sub>(μ-SEt)<sub>2</sub>](SEt)<sub>4</sub>]<sup>2–</sup>:<sup>11</sup> mean Fe–S<sub>μ</sub>, 2.375(1); Fe•••Fe, 2.978(1); S<sub>μ</sub>–Fe–S<sub>μ</sub>, 102.3(1); Fe–S<sub>μ</sub>–Fe, 77.7(1). (b) [Fe{N(SiMe<sub>3</sub>)<sub>2</sub>}{μ-SC<sub>6</sub>H<sub>3</sub>-2,6-(SiMe<sub>3</sub>)<sub>2</sub>}]<sub>2</sub>:<sup>12</sup> mean Fe–N, 1.89(1); mean Fe–S, 2.37(3); mean Fe•••Fe, 3.687(2); mean S–Fe–S, 78(2); mean Fe–S–Fe, 102(1).

(11) Hagen, K. S.; Holm, R. H. *Inorg. Chem.* **1984**, *23*, 418.  
(12) Hauptmann, R.; Kliss, R.; Schneider, J.; Henkel, G. *Z. Anorg. Allg. Chem.* **1998**, *624*, 1927.

(13) Ellison, J. J.; Senge, K. R.; Power, P. P. *Angew. Chem., Int. Ed. Engl.* **1994**, *33*, 1178.

(1) For a recent series of comprehensive reviews, see: (a) Howard, J. B.; Rees, D. C. *Chem. Rev.* **1996**, *96*, 2965. (b) Burgess, B. K.; Lowe, D. J. *Chem. Rev.* **1996**, *96*, 2983. (c) Eady, R. R. *Chem. Rev.* **1996**, *96*, 3013.

(2) (a) Chan, M. K.; Kim, J.; Rees, D. C. *Science* **1993**, *260*, 792. (b) Kim, J.; Woo, D.; Rees, D. C. *Biochemistry* **1993**, *32*, 7104. (c) Bolin, J. T.; Campobasso, N.; Muchmore, S. W.; Morgan, T. V.; Mortenson, L. E. In *Molybdenum Enzymes, Cofactors, and Model Systems*; Stiefel, E. I., Coucouvanis, D., Newton, W. E., Eds.; ACS Symp. Ser. No. 535; American Chemical Society: Washington, DC, 1993; pp 186–195.

(3) (a) Thorneley, R. N. F.; Lowe, D. J. *J. Biol. Inorg. Chem.* **1996**, *1*, 576. (b) Dance, I. *J. Biol. Inorg. Chem.* **1996**, *1*, 581. (c) Sellmann, D.; Sutter, J. *J. Biol. Inorg. Chem.* **1996**, *1*, 587. (d) Coucouvanis, D. *J. Biol. Inorg. Chem.* **1996**, *1*, 594. (e) Pickett, C. J. *J. Biol. Inorg. Chem.* **1996**, *1*, 601. (f) Leigh, G. J. *Eur. J. Biochem.* **1995**, *535*, 171.

(4) (a) Rod, T. H.; Hammer, B.; Nørskov, J. K. *Phys. Rev. Lett.* **1999**, *82*, 4054. (b) Dance, I. *Chem. Commun.* **1998**, 523. (c) Siegbahn, P. E. M.; Westerberg, J.; Svensson, M.; Crabtree, R. H. *J. Phys. Chem. B* **1998**, *102*, 1615. (d) Stavrev, K. K.; Zerner, M. C. *Int. J. Quantum Chem.* **1998**, *70*, 1159. (e) Dance, I. *Chem. Commun.* **1997**, 165. (f) Zhong, S.-J.; Liu, C.-W. *Polyhedron* **1997**, *16*, 653. (g) Shestakov, A. F. *Russ. Chem. Bull.* **1996**, *45*, 1827. (h) Stavrev, K. K.; Zerner, M. C. *Chem. Eur. J.* **1996**, *2*, 83. (i) Machado, F. B. C.; Davidson, E. R. *Theor. Chim. Acta* **1995**, *92*, 315. (j) Dance, I. G. *Aust. J. Chem.* **1994**, *47*, 979. (k) Plass, W. *J. Mol. Struct.* **1994**, *315*, 53. (l) Deeth, R. J.; Field, C. N. *J. Chem. Soc., Dalton Trans.* **1994**, 1943. (m) Hoffmann, R.; Deng, H. *Angew. Chem., Int. Ed. Engl.* **1993**, *32*, 1062.

(5) (a) Anderson, R. A.; Faegri, K., Jr.; Green, J. C.; Haaland, A.; Lappert, M. F.; Leung, W.-P.; Rydpal, K. *Inorg. Chem.* **1988**, *27*, 1782. (b) Olmstead, M. M.; Power, P. P.; Shoner, S. C. *Inorg. Chem.* **1991**, *30*, 2547.

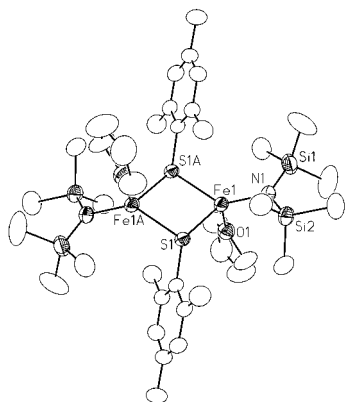


**Figure 1.** Structure of  $[\text{Fe}\{\text{N}(\text{SiMe}_3)_2\}(\mu\text{-SMes})(\text{THF})_2]$  (**1a-THF**) with thermal ellipsoids (35% probability level) and selected atom labels; hydrogens are omitted for clarity. Selected distances (Å) and angles (deg): Fe1–N1, 1.934(2); Fe1–S1, 2.4296(8); Fe1–S1A, 2.3846(8); Fe1–O1, 2.113(2); Fe1⋯Fe1A, 3.534(1); S1–Fe1–S1A, 85.55(3); N1–Fe1–O1, 105.96(10); N1–Fe1–S1A, 135.01(8); O1–Fe1–S1A, 101.12(7); N1–Fe1–S1, 119.31(8); O1–Fe1–S1, 106.11(6); Fe1–S1–Fe1A, 94.45(3).

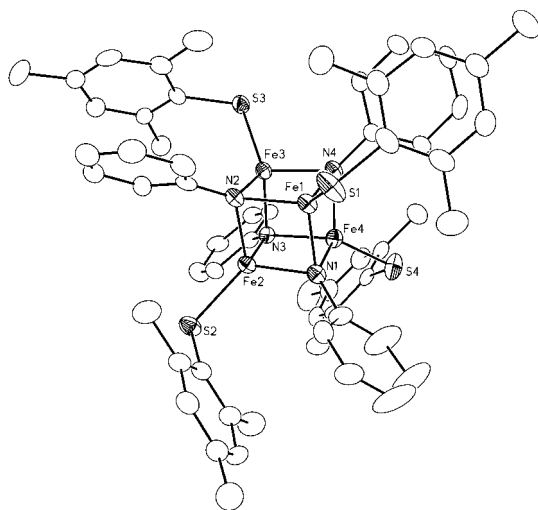


**Figure 2.** Structure of  $[\text{Fe}_4(\mu_3\text{-NPh})_4(\text{SMes})_4]$  (**2a**) with thermal ellipsoids (35% probability level) and selected atom labels; hydrogens are omitted for clarity. One of two independent molecules is shown. Selected distance (Å) and angle (deg) ranges [mean]: Fe–N, 1.941(5)–1.985(5) [1.96(1)]; Fe–S, 2.200(2)–2.225(2) [2.214(9)]; Fe⋯Fe, 2.593(2)–2.666(1) [2.63(2)]; N–Fe–N, 94.4(2)–97.1(2) [95.4(7)]; Fe–N–Fe, 82.9(2)–85.2(2) [84.3(6)]; S–Fe–N, 114.6(2)–127.6(2) [121(3)].

(**2a**) as dark brown microcrystals in 60% isolated yield.<sup>14</sup> The reaction proceeds well for aryl thiols with moderately bulky 2,6-substituents (Me, *i*Pr). The yields, however, drop substantially for the more hindered TriphSH, while the reaction with unhindered benzenethiol forms a dark, soluble material, as yet unidentified, which does not appear to be tetranuclear cluster **2**.

Large diffraction-quality crystals of **2a** were obtained from benzene solutions doped with *n*-pentane by slow evaporation at  $-25^\circ\text{C}$ . X-ray analysis of **2a** reveals a cluster with four equivalent tetrahedral iron centers, each terminally ligated by thiolate and bridged by three phenyl imido ligands to form an  $[\text{Fe}_4(\mu_3\text{-NPh})_4]^{4+}$  (all ferric) cubane core (Figure 2).<sup>9b</sup> Two nearly identical, independent molecules of **2a**, each with approximate  $C_2$  symmetry (including pendant aryl rings), occupy the asymmetric unit. In solution, the complex displays a characteristic paramagnetic  $^1\text{H}$

(14)  $^1\text{H}$  NMR (500 MHz,  $\text{C}_6\text{D}_6$ , 293 K):  $\delta$  13.54 (8 H, *m*-Ph), 11.77 (8 H, *m*-Mes), 5.49 (24 H, *o*-Me), 5.02 (12 H, *p*-Me), 0.59 (8 H, *o*-Ph),  $-1.06$  (4 H, *p*-Ph). Anion-mode laser desorption/ionization mass spectrum (LDI-TOF MS):  $m/z$  1192.4 (theoretical 1192.8).

NMR spectrum consistent with rapid ring rotation and idealized  $T_d$  molecular symmetry.<sup>14</sup> Compound **2** is also characterized by a prominent parent ion signal in anion-mode LDI-TOF MS.<sup>14</sup> Variable-temperature magnetic susceptibility measurements show Curie–Weiss law behavior below 30 K which fits an  $S = 2$  ground electronic state.<sup>15</sup> The complex is stable only in relatively inert solvents (hydrocarbons, arenes, ethers) and decomposes within minutes upon exposure of a solid sample to air. Cluster **2a** represents one of the few structurally characterized examples of a transition series  $[\text{M}_4(\mu_3\text{-NR})_4]$  cubane core,<sup>16</sup> and the first case with nonorganometallic, weak-field ligation. The mixed cubane  $[\text{Fe}_4(\mu_3\text{-S})_2(\mu_3\text{-N}^t\text{Bu})_2](\text{NO})_4$ , prepared by reaction of  $\text{Hg}[\text{Fe}(\text{CO})_3(\text{NO})_2]$  with  $(^t\text{BuN})_2\text{S}$ , is perhaps the closest structural analogue to **2**;<sup>17</sup> however, the electronic properties of the two clusters—strong field  $\text{Fe}^{1+}$  with metal–metal bonding vs weak field, high spin  $\text{Fe}^{3+}$ —differ considerably. Equivalent core interatomic distances<sup>18</sup> are consistently longer for **2a**, in keeping with its formulation as a high-spin cluster.

The assembly of cluster **2** via reductive scission (or, equivalently, oxidative addition) of a N–N bond is noteworthy.<sup>19</sup> Cleavage of azo (RN=NR) substrates has been observed in low-valent iron carbonyl cluster chemistry,<sup>20</sup> but to our knowledge, this is the first documented example of a hydrazine cleavage coupled to ferrous/ferric oxidation.<sup>21</sup> The imido ligands in the core of cluster **2a** are accessible: stoichiometric addition of *p*-toluidine results, within minutes, in exchange of the free toluidine with the phenyl imido bridges (as monitored by NMR and LDI MS) without cluster decomposition. To the extent that fundamental reaction chemistry can suggest plausible enzyme mechanisms, our present study advances the possibility of discrete, core-bound nitrogen within the cofactor cluster as a ligation mode following  $\text{N}_2$  scission and preceding ammonia evolution.

The synthesis of **2** provides an opportunity to examine both a transformation and resultant cluster product which are chemically related to recent proposals for nitrogenase mechanism. Future reports will describe further investigations into the reaction chemistry of iron, nitrogen, and sulfur.

**Acknowledgment.** We thank the Arnold and Mabel Beckman Foundation (Beckman Young Investigator Award) for their generous support.

**Supporting Information Available:** Crystallographic data for compounds **1a-THF** and **2a** and NMR data for  $[\text{Fe}(\mu\text{-STriph})\{\text{N}(\text{SiMe}_3)_2\}]_2$  and  $[\text{Fe}(\mu\text{-STriph})(\text{STriph})_2]$  (PDF). This material is available free of charge via the Internet at <http://pubs.acs.org>.

JA9919783

(15) For  $T = 4\text{--}30\text{ K}$ ,  $\chi^M = C/(T - \theta)$ , where  $C = 2.77\text{ emu}\cdot\text{K}/\text{mol}$ ,  $\theta = -3.68\text{ K}$ ; for an ideal  $S = 2$  system, the Curie constant  $C = 3.00\text{ emu}\cdot\text{K}/\text{mol}$ , assuming  $g_e = 2$ .

(16) (a)  $[\text{Co}_4(\mu_3\text{-N}^t\text{Bu})_4](\text{NO})_4$ : Gall, R. S.; Connelly, N. G.; Dahl, L. F. *J. Am. Chem. Soc.* **1974**, *96*, 4017. (b)  $[\text{CpTi}(\mu_3\text{-NSnMe}_3)_4]$ : Decker, A.; Fenske, D.; Maczek, K. *Angew. Chem., Int. Ed. Engl.* **1996**, *35*, 2863.

(17) (a) Gall, R. S.; Chu, C. T.-W.; Dahl, L. F. *J. Am. Chem. Soc.* **1974**, *96*, 4019. (b) Chu, C. T.-W.; Gall, R. S.; Dahl, L. F. *J. Am. Chem. Soc.* **1982**, *104*, 737.

(18) Selected distances (Å) and angles (deg) for  $[\text{Fe}_4(\mu_3\text{-S})_2(\mu_3\text{-N}^t\text{Bu})_2](\text{NO})_4$ :<sup>17b</sup> mean Fe–N, 1.910(5); Fe⋯Fe (for  $\text{Fe}_2\text{N}_2$  face), 2.496(1); N–Fe–N, 98.0(2); Fe–N–Fe, 81.6(1).

(19) Metal-mediated N–N/N=N bond activation is a topic of current interest; for some recent examples, see: (a) Peters, R. G.; Warner, B. P.; Burns, C. J. *J. Am. Chem. Soc.* **1999**, *121*, 5585. (b) Aubert, M. A.; Bergman, R. G. *Organometallics* **1999**, *18*, 811. (c) Kaplan, A. W.; Polse, J. L.; Ball, G. E.; Anderson, R. A.; Bergman, R. G. *J. Am. Chem. Soc.* **1998**, *120*, 11649. (d) Maseras, F.; Lockwood, M. A.; Eisenstein, O.; Rothwell, I. P. *J. Am. Chem. Soc.* **1998**, *120*, 6598.

(20) (a) Wucherer, E. J.; Tasi, M.; Hansert, B.; Powell, A. K.; Garland, M.-T.; Halet, J.-F.; Saillard, J.-Y.; Vahrenkamp, H. *Inorg. Chem.* **1989**, *28*, 3564. (b) Hansert, B.; Vahrenkamp, H. *J. Organomet. Chem.* **1993**, *460*, C19. (c) Kabir, S. E.; Ruf, M.; Vahrenkamp, H. *J. Organomet. Chem.* **1998**, *571*, 91 and references therein.

(21) Heterometal  $[\text{MFe}_3\text{S}_4]$  cubanes (M = Mo, V) have been found to catalyze the reductive cleavage of hydrazine to ammonia, while all-iron  $[\text{Fe}_4\text{S}_4]$  cubanes do not; the heterometal has been implicated as the reaction site in these systems.<sup>3c</sup>